JACS ARTICLES

Published on Web 08/20/2010

Ultrasmall Titania Nanocrystals and Their Direct Assembly into Mesoporous Structures Showing Fast Lithium Insertion

Johann M. Szeifert,[†] Johann M. Feckl,[†] Dina Fattakhova-Rohlfing,[†] Yujing Liu,[†] Vit Kalousek,[‡] Jiri Rathousky,[‡] and Thomas Bein*[,†]

Department of Chemistry and Center for NanoScience (CeNS), University of Munich (LMU), Munich, Germany, and J. Heyrovský Institute of Physical Chemistry, Academy of Sciences of the Czech Republic, Prague, Czech Republic

Received March 3, 2010; E-mail: bein@lmu.de

Abstract: Ultrasmall and highly soluble anatase nanoparticles were synthesized from $TiCl_4$ using *tert*-butyl alcohol as a new reaction medium. This synthetic protocol widens the scope of nonaqueous sol−gel methods to TiO_2 nanoparticles of around 3 nm with excellent dispersibility in ethanol and *tert*-butanol. Microwave heating was found to enhance the crystallinity of the nanoparticles and to drastically shorten the reaction time to less than 1 h at temperatures as low as 50 °C. The extremely small size of the nanoparticles and their dispersibility make it possible to use commercial Pluronic surfactants for evaporation-induced self-assembly of the nanoparticulate building blocks into periodic mesoporous structures. A solution of particles after synthesis can be directly used for preparation of mesoporous films without the need for particle separation. The mesoporous titania coatings fabricated using this one-pot procedure are crystalline and exhibit high surface areas of up to 300 m^2/g. The advantages of the retention of the mesoporous order with extremely thin nanocrystalline walls were shown by electrochemical lithium insertion. The films made using microwave-treated nanoparticles showed supercapacitive behavior with high maximum capacitance due to quantitative lithiation with a 10-fold increase of charging rates compared to a standard reference electrode made from 20 nm anatase particles.

Introduction

Mesoporous crystalline metal oxide layers have been the focus of extensive research activities for the past decade.[1−5] The crystallinity of a metal oxide scaffold in combination with a high interfacial surface area and a periodic ordering on the nanoscale is of special interest in applications involving interfacial charge transfer and bulk charge transport processes such as solar cells,[6−8] sensors,[9] and energy storage devices.[10,11] The basic approach to manufacturing such layers is the self-assembly of metal oxide building units assisted by a suitable structure-directing agent.[1,12] The critical point here is the amorphous character of the common metal oxide precursors, which usually emanate from sol−gel synthesis and require crystallization at elevated temperatures, often resulting in the collapse of the mesostructure.[13] This limitation motivates the search for largely crystalline building units that could convert to the final crystalline periodic scaffolds under mild conditions and low temperatures.[14] To make such an approach successful, the building blocks need to be extremely small in order to be compatible with the size of the structure-directing agents, and they should be dispersible in the required solvents without agglomeration.[15] Hydrothermal synthesis methods are often unsuitable for this purpose due to the fast reaction rates, resulting in highly agglomerated nanoparticles with a wide distribution of particle size and shape. On the contrary, nonaqueous solvothermal routes usually provide much better control over the size, crystallinity, and agglomeration behavior of the nanoparticles.[16] Among the large number of organic solvents examined in this context, benzyl alcohol has received much

[†] University of Munich.
[‡] Academy of Sciences of the Czech Republic.

(1) Yang, P.; Zhao, D.; Margolese, D. I.; Chmelka, B. F.; Stucky, G. D. *Nature* **1998**, *396*, 152–155.
(2) Lee, J.; Orilall, C. M.; Warren, S. C.; Kamperman, M.; DiSalvo, F. J.; Wiesner, U. *Nat. Mater.* **2008**, *7*, 222–228.
(3) Boettcher, S. W.; Fan, J.; Tsung, C.-K.; Shi, Q.; Stucky, G. D. *Acc. Chem. Res.* **2007**, *40*, 784–792.
(4) Wan, Y.; Yang, H.; Zhao, D. *Acc. Chem. Res.* **2006**, *39*, 423–432.
(5) Sanchez, C.; Boissière, C.; Grosso, D.; Laberty, C.; Nicole, L. *Chem. Mater.* **2008**, *20*, 682–737.
(6) O'Regan, B.; Gratzel, M. *Nature* **1991**, *353*, 737–740.
(7) Zhang, Q.; Chou, T. P.; Russo, B.; Jenekhe, S. A.; Cao, G. *Angew. Chem., Int. Ed.* **2008**, *47*, 2402–2406.
(8) Rajan, J.; Velmurugan, T.; Seeram, R. *J. Am. Ceram. Soc.* **2009**, *92*, 289–301.
(9) Pinna, N.; Neri, G.; Antonietti, M.; Niederberger, M. *Angew. Chem., Int. Ed.* **2004**, *43*, 4345–4349.
(10) Li, H.; Balaya, P.; Maier, J. *J. Electrochem. Soc.* **2004**, *151*, A1878–A1885.
(11) Poizot, P.; Laruelle, S.; Grugeon, S.; Dupont, L.; Tarascon, J. M. *Nature* **2000**, *407*, 496–499.
(12) Grosso, D.; Cagnol, F.; Soler-Illia, G. J. de A. A.; Crepaldi, E. L.; Amenitsch, H.; Brunet-Bruneau, A.; Bourgeois, A.; Sanchez, C. *Adv. Funct. Mater.* **2004**, *14*, 309–322.
(13) Yang, P.; Zhao, D.; Margolese, D. I.; Chmelka, B. F.; Stucky, G. D. *Chem. Mater.* **1999**, *11*, 2813–2826.
(14) Szeifert, J. M.; Fattakhova-Rohlfing, D.; Georgiadou, D.; Kalousek, V.; Rathousky, J.; Kuang, D.; Wenger, S.; Zakeeruddin, S. M.; Gratzel, M.; Bein, T. *Chem. Mater.* **2009**, *21*, 1260–1265.
(15) Fattakhova-Rohlfing, D.; Szeifert, J. M.; Yu, Q.; Kalousek, V.; Rathousky, J.; Bein, T. *Chem. Mater.* **2009**, *21*, 2410–2417.
(16) Niederberger, M.; Garnweitner, G. *Chem.—Eur. J.* **2006**, *12*, 7282–7302.

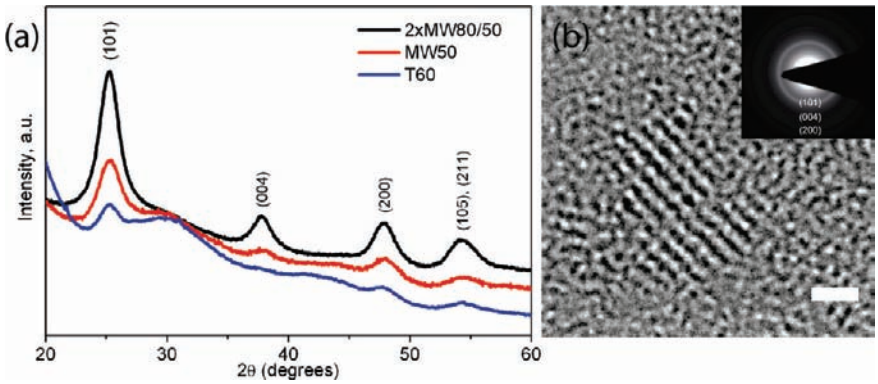

Figure 1. Crystallinity and morphology of the TiO_2 nanoparticles obtained using *tert*-BuOH as the reaction medium after different synthesis conditions: WAXS patterns of samples T60 (blue), MW50 (red), and 2xMW80/50 (black) (a); high resolution TEM image (HRTEM) and SAED pattern (inset) of the MW50 particles (b). The scale bar corresponds to a distance of 1.0 nm.

attention, as it enables the synthesis of a large variety of metal oxide nanoparticles with high crystallinity, a low degree of agglomeration, and tunable particle size.[17,18] However, it is difficult to prepare extremely small particles with this approach, and surface-modifying ligands are needed for stabilization. Another issue with the benzyl alcohol synthesis is the presence of benzyl alcoholate residues on the particles' surface, which influence physical and chemical properties of the interface and can be removed only by harsh oxidative treatment or at temperatures above 450 °C.[19,20] An accessible and ligand-free surface is, however, of great importance for charge transfer processes across the interfaces. This issue can be solved when nonaromatic solvents are used as reaction medium.[21] Thus, polyols enable the preparation of monodisperse crystalline nanoparticles with good interface properties; however, again it is difficult to prepare very small nanoparticles with this approach.[22,23] Aliphatic alcohols usually require higher reaction temperatures and typically do not provide homodispersed nonagglomerated nanocrystals.[24−27] Crystalline nanoparticles can also be prepared in other nonaqueous solvents such as ketones or aldehydes.[28]

Aiming to prepare metal oxide nanoparticles of small size, enhanced crystallinity and good dispersibility without the need of additional stabilizing ligands, we explored *tert*-butanol as a novel reaction medium. Similar to other small aliphatic alcohols, this solvent can be easily removed due to its low boiling point of 83 °C. The unique reactivity of *tert*-butanol resulting from a strong inductive stabilization of an intermediate carbocation is supposed to result in a different mechanism of particle formation compared to that of other aliphatic alcohols, thus leading to particles with different properties and morphology.[29] As a metal oxide system we selected titanium dioxide, which is of great interest for applications in solar cells, catalysis, and energy storage.[30]

Here we describe the use of *tert*-butanol as a new solvent and reactant in a nonaqueous sol−gel protocol leading to highly dispersible and nanocrystalline titania particles without the need for additional ligands or surfactants. Ultrasmall anatase nanoparticles of high crystallinity were obtained by a special microwave-based heating procedure that allows the crystal formation within several minutes. Additionally, this new approach permits the direct application of the as-synthesized particles in combination with a commercial polymer template for the preparation of mesoporous titanium dioxide films without the need for particle separation or chemical processing. The crystalline nature of the films and their use as electrode material for Li-ion batteries is shown by electrochemical lithium insertion. Here, the high surface to bulk ratio of the nanocrystals and the easily accessible mesoporous structures with extremely thin walls lead to a drastic acceleration of the Li insertion and high maximum capacitance. Our synthetic strategy leading to highly dispersible and crystalline nanoparticles represents a versatile alternative for the preparation of periodically ordered mesostructures and should be applicable to other metal oxides and mixed oxides.

Results and Discussion

In a typical procedure for the preparation of titanium dioxide nanoparticles, a solution of titanium tetrachloride in toluene was added to water-free *tert*-butanol at 25 °C and subjected to different temperature treatments. In a conventional synthesis, the reaction mixture was put into an oven at 60 °C for 24 h until it turned into a colorless but turbid and highly viscous suspension (assigned further as T60). After cooling to room temperature, the nanoparticles were separated by centrifugation for further characterization. The particles were highly dispersible in ethanol, and wide-angle X-ray scattering (WAXS) of the material showed the formation of partially crystalline TiO_2 anatase particles of about 4 nm in size and the presence of a relatively large amount of amorphous phase (Figure 1a).

(17) Niederberger, M.; Bartl, M. H.; Stucky, G. D. *Chem. Mater.* **2002**, *14*, 4364–4370.
(18) Niederberger, M.; Bartl, M. H.; Stucky, G. D. *J. Am. Chem. Soc.* **2002**, *124*, 13642–13643.
(19) Niederberger, M.; Garnweitner, G.; Krumeich, F.; Nesper, R.; Colfen, H.; Antonietti, M. *Chem. Mater.* **2004**, *16*, 1202–1208.
(20) Kotsokechagia, T.; Cellesi, F.; Thomas, A.; Niederberger, M.; Tirelli, N. *Langmuir* **2008**, *24*, 6988–6997.
(21) Pinna, N.; Niederberger, M. *Angew. Chem., Int. Ed.* **2008**, *47*, 5292–5304.
(22) Feldmann, C.; Jungk, H.-O. *Angew. Chem., Int. Ed.* **2001**, *40*, 359–362.
(23) Feldmann, C. *Adv. Funct. Mater.* **2003**, *13*, 101–107.
(24) Wang, C.; Deng, Z.-X.; Zhang, G.; Fan, S.; Li, Y. *Powder Technol.* **2002**, *125*, 39–44.
(25) Yang, X.; Konishi, H.; Xu, H.; Wu, M. *Eur. J. Inorg. Chem.* **2006**, *2006*, 2229–2235.
(26) Li, G.; Li, L.; Boerio-Goates, J.; Woodfield, B. F. *J. Am. Chem. Soc.* **2005**, *127*, 8659–8666.
(27) Wang, C.; Deng, Z.-X.; Li, Y. *Inorg. Chem.* **2001**, *40*, 5210–5214.
(28) Garnweitner, G.; Antonietti, M.; Niederberger, M. *Chem. Commun.* **2005**, 397–399.
(29) Kominami, H.; Kato, J.; Takada, Y.; Doushi, Y.; Ohtani, B.; Nishimoto, S.; Inoue, M.; Inui, T.; Kera, Y. *Catal. Lett.* **1997**, *46*, 235–240.
(30) Bartl, M. H.; Boettcher, S. W.; Frindell, K. L.; Stucky, G. D. *Acc. Chem. Res.* **2005**, *38*, 263–271.

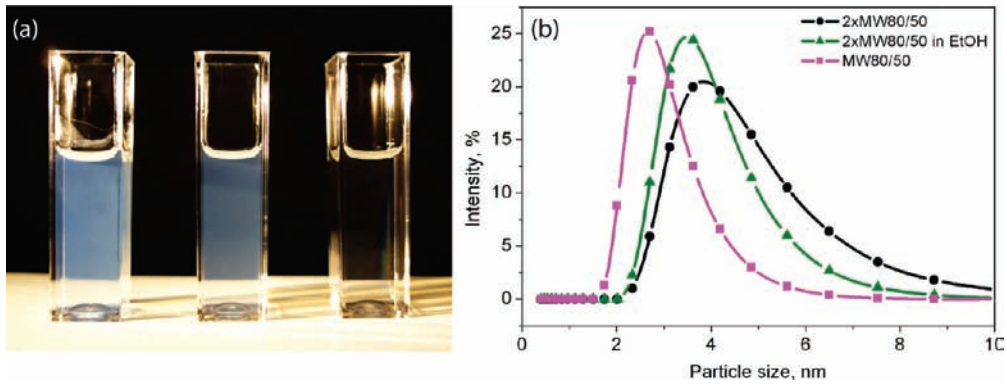

Figure 2. (a) Picture of 2xMW80/50 particle solutions: in *tert*-butanol/toluene (3:1 volume ratio, 3.3 wt % TiO_2, left), after flocculation with heptane, centrifugation, and redispersion in ethanol (3.3 wt %, middle), and further diluted in ethanol (0.7 wt %, right). (b) DLS data of dispersions of particles prepared by microwave treatment in *t*BuOH (magenta: MW80/50, black: 2xMW80/50) and of 2xMW80/50 in EtOH (green).

In an attempt to shorten the reaction time, microwave-based heating was examined for this reaction mixture, as it had been reported for other systems to significantly accelerate certain reactions.[31] After only 1 h at 50 °C under microwave irradiation, the solution turned colorless and transparent, and formation of anatase particles of only 3.1 nm was observed by dynamic light scattering (DLS) and WAXS (Sample MW50, Figure 1a). The broad background in the WAXS pattern still indicates the presence of amorphous material, but at much lower relative ratios than those for samples prepared by conventional heating. Microwave syntheses at higher temperatures led not only to a significant increase in crystallinity but also to larger particle sizes and precipitation of the particles from the solution, thus decreasing their dispersibility.

Using microwave irradiation, we aimed to maximize the yield of crystalline material in the product and simultaneously to prevent further particle growth and agglomeration. For this purpose, we combined a fast ramp to a higher temperature such as 80 °C for an initial burst of nucleation, directly followed by a cooling period and a longer dwell time at lower temperatures (50 °C) for subsequent particle growth (sample MW80/50). This procedure leads to the formation of very small and crystalline particles without visible agglomeration, as demonstrated by the DLS data of the particles in solution (Figure 2) and the transmission electron microscopy (TEM) images of dried particles on a carbon-coated copper grid (Figure 1b). Although DLS data show the formation of small particles of less than 3 nm in size, the yellow color of the reaction solution still indicates the presence of titanium-chloro complexes and thus incompletely reacted molecular precursors. It was found that after two cycles of this heat treatment a colorless and slightly turbid solution can be obtained (sample 2xMW80/50), from which nanoscale titanium dioxide could be flocculated using *n*-heptane. TGA data of this sample show weight loss to above 400 °C, suggesting the presence of organic material on the surface of the nanoparticles (Supporting Information Figure S1). The WAXS pattern of particles made this way shows much reduced amorphous phase, and the peak broadening corresponds to nanocrystals of 3.8 nm in size (Figure 1a). This is in good agreement with the HRTEM micrographs (Figure 1b) that show particles of the same size exhibiting lattice fringes and the typical *d*-spacings and electron diffraction pattern of anatase.

The dispersibility of the particles in *tert*-butanol and ethanol was proven by DLS, showing monodisperse particles with hydrodynamic radii of about 3 to 4 nm (Figure 2).

The excellent dispersibility of the *tert*-butanol-based nanoparticles in both ethanol and *tert*-butanol can be exploited for the preparation of mesoporous films using the as-synthesized nanocrystals as metal oxide building blocks. The special advantages of *tert*-butanol are, first, that due to its low boiling point of only 83 °C, unlike benzyl alcohol, it is a suitably volatile solvent for evaporation-induced self-assembly (EISA) in thin films. Second, it is a good solvent for the polymers of the Pluronic family, which are commonly used as templates for mesostructure formation.[3,30] Therefore, the reaction mixture containing the nanoparticles can be used directly, and the effort needed for the additional steps of particle separation and redispersion in other solvents suitable for the EISA process can be avoided. Using this direct coating technique, mesoporous titanium dioxide films were produced from solutions containing Pluronic P123 in *tert*-butanol that were treated with either one cycle of microwave irradiation or two microwave cycles and thus containing fully crystalline titania particles. For comparison, films were also prepared without any heat treatment of the coating solution from a sol−gel precursor in *tert*-butanol (sample tBuOH-SG).

A TEM investigation of very thin films was performed to gain insights into how the particles arrange around the pores forming the network. The contrast variations in the walls around the mesopores in Figure 3b and 3c prove that, for both microwave-heated samples, the pore walls consist of many small particles, whereas, for the untreated solution, the walls surrounding the pores show uniform density which indicates the presence of homogeneous but amorphous titanium dioxide (Figure 3a). The tBuOH-SG sample also exhibits a worm-like pore structure, which only converts to an open porous phase at higher temperatures as observed by SEM after calcination at 300 °C (Figure 3d and Supporting Information Figure S2).

All of the layers prepared from different types of reaction mixtures and calcined at 300 °C show mesoporous structures with a regular, wormlike pore system. The reference sample prepared from nontreated sol−gel titania precursor (Figure 3d) exhibits the highest degree of periodicity, the largest size of periodic domains, and the smallest mesostructure spacing of 14 nm. The MW80/50 particle solution results in a structure with slightly smaller periodic domains and a larger pore spacing of about 20 nm (Figure 3e), while the use of a solution with

(31) Bilecka, I.; Djerdj, I.; Niederberger, M. *Chem. Commun.* **2008**, 886–888.

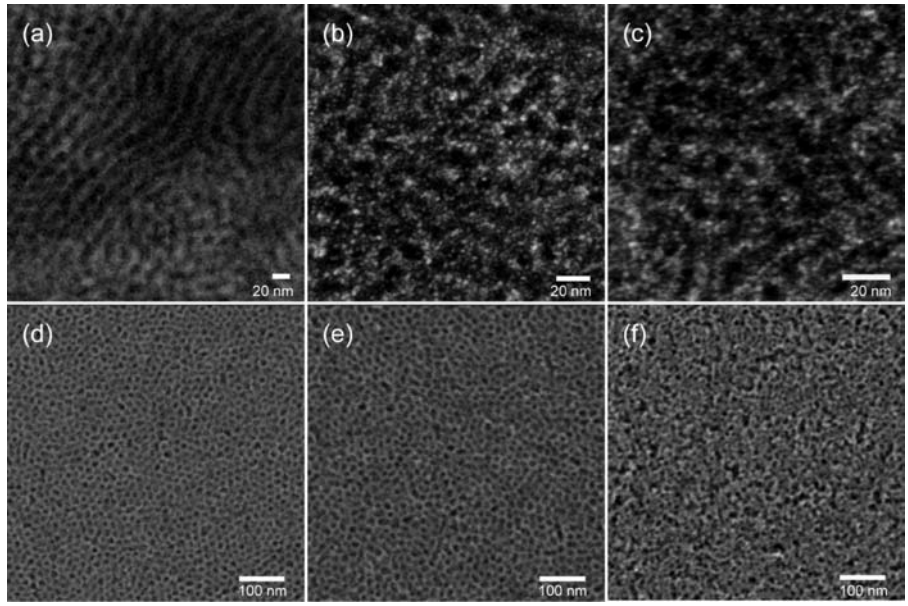

Figure 3. Mesoporous titanium dioxide films assembled from different building blocks: *tert*-butanol titania sol−gel (tBuOH-SG) (a, d), MW80/50 (b, e), and 2xMW80/50 (c, f). The first row (a−c) shows STEM-HAADF images of the films directly after coating, and the second row (d−f) SEM images (top view) of the same films after calcination at 300 °C.

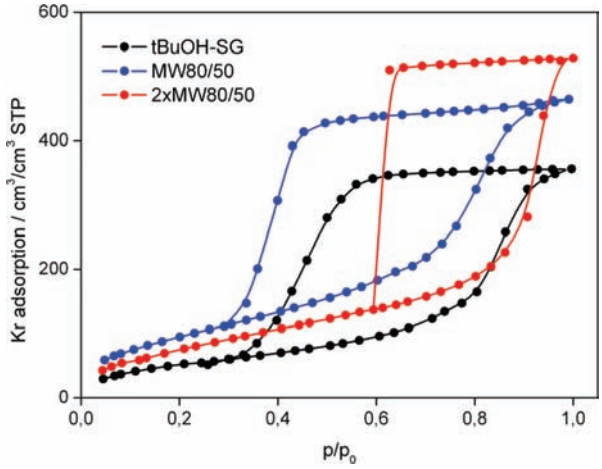

Figure 4. Isotherms of Krypton adsorption on the titania layers assembled from different building blocks: tBuOH-SG (black), MW80/50 (blue), 2xMW80/50 (red). The BET surface areas of these films are 116 m^2/g (tBuOH-SG), 294 m^2/g (MW80/50), and 297 m^2/g (2xMW80/50). The films were calcined at 300 °C.

the more crystalline 2xMW80/50 particles leads to a much less periodic structure on the film surface (Figure 3f). Still, pores of the same size that are open to the surface can be observed.

The mesoporous nature of the pore system after the template combustion was also investigated using Kr adsorption (Figure 4, and Supporting Information Figure S3). The isotherms of all layers exhibit the typical shape of mesoporous materials with a large surface area, high pore volume, and the open and accessible character of porosity. The highest surface area of about 300 m^2/g is exhibited by the layers assembled from the MW80/50 and 2xMW80/50 particles. The use of more crystalline 2xMW80/50 particles leads to mesoporous layers with increased pore size and pore volume. The periodicity of the mesostructure after treatment at high temperatures was confirmed by the existence of reflections in small-angle X-ray scattering (SAXS; see Supporting Information Figure S4) from samples calcined at different temperatures. At room temperature, the samples exhibited the typical reflection of Pluronic P123-templated titania corresponding to *d*-spacings of 10 to 12 nm. After calcination at 450 °C, this peak was shifted to higher angles and gradually disappeared at higher temperatures due to the rather strong contraction of the mesostructure in the direction perpendicular to the substrate.[32,33] At the same time, other reflections became visible close to the lower detection limit of the SAXS at 0.6° to 0.7° 2θ and remained at the same position upon further heating. This proves the existence of periodically repeating structural features after heating up to 600 °C and indicates structural changes upon thermal treatment.

The crystallization behavior upon heating was also monitored by evaluating the peak broadening in wide-angle X-ray scattering (WAXS). In the sol−gel sample (tBuOH-SG), first traces of anatase nanoparticles of about 4.7 nm could be detected only after heating to 450 °C (Figure 5 and Supporting Information Figure S5).[33,34] At even higher temperatures, the nanocrystals in the *tert*-butanol sol−gel sample grow rapidly and almost triple their size when heated to 600 °C. The microwave-treated nanoparticulate precursor, however, exhibits a more steady, controllable crystallization, and the particles of originally 4 nm grow to only about 6 nm at 300 °C, to 8 nm at 500 °C, and finally to 11 to 13 nm at 600 °C. In summary, at 450 °C the nanoparticulate systems show both crystallinity and templated mesoporosity, while the sol−gel derived systems show only low crystallinity with templated mesoporosity. On heating to 600 °C, both systems have lost the templated mesoporosity due to further crystal growth.

Electrochemical lithium insertion was performed for the determination of the relative amounts of crystalline and amorphous phase in the films assembled from different precursors and to examine their applicability as electrode materials for Li-

(32) Grosso, D.; Soler-Illia, G. J. d. A. A.; Crepaldi, E. L.; Cagnol, F.; Sinturel, C.; Bourgeois, A.; Brunet-Bruneau, A.; Amenitsch, H.; Albouy, P. A.; Sanchez, C. *Chem. Mater.* **2003**, *15*, 4562–4570.
(33) Crepaldi, E. L.; Soler-Illia, G. J. d. A. A.; Grosso, D.; Cagnol, F.; Ribot, F.; Sanchez, C. *J. Am. Chem. Soc.* **2003**, *125*, 9770–9786.
(34) Choi, S. Y.; Mamak, M.; Speakman, S.; Chopra, N.; Ozin, G. A. *Small* **2005**, *1*, 226–232.

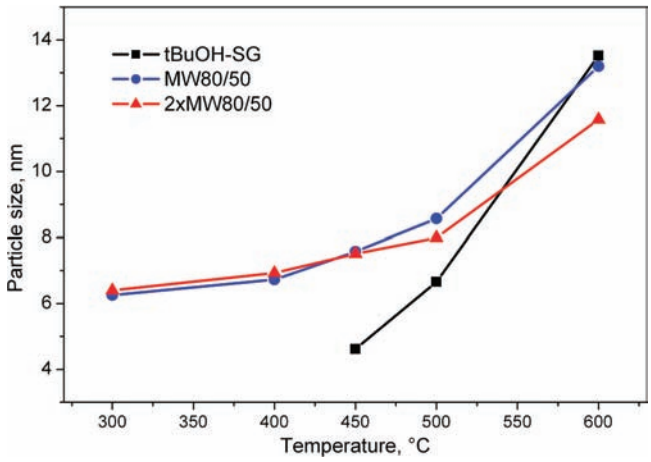

Figure 5. Development of crystal size from broadening of the (101) anatase reflection in wide-angle X-ray scattering upon heating. Black: tBuOH-SG, blue: MW80/50, red: 2xMW80/50 (film data below 300 °C were not recorded due to their low scattering intensity).

ion batteries.[35,36] The layers were calcined at 300 °C in order to combust the template and to open the pores and, at 450 °C, to induce further crystallization of the networks. Cyclic voltammograms of the films prepared from the untreated solution exhibit only the broad insertion/extraction features of the amorphous phase even after calcination at 450 °C (Figure 6). The films prepared from the MW80/50 nanoparticles show the insertion behavior of an amorphous titania phase after calcination at 300 °C and, after calcination at 450 °C, clearly feature the characteristic quasireversible insertion/extraction anatase-based peaks around 1.85 V vs Li. Finally, the films assembled from 2xMW80/50 particles show the presence of anatase already after calcination at 300 °C. The amount of crystalline anatase phase doubles after heating the films at 450 °C, and only small traces of TiO_2(B) (around 1.6 V) are observable.

The above evidence shows that the microwave irradiation of the titanium tetrachloride solution in *tert*-butanol leads to the formation of ultrasmall crystalline nanoparticulate seeds, which after film preparation can induce crystallization of the surrounding network at elevated temperatures by lowering the activation energy.

The films from solutions employing two cycles of the burst of nucleation profile (sample 2xMW80/50) show a capacity for lithium insertion at 1.7 V (end of the first plateau corresponding to insertion into anatase) of 143 mAh/g after calcination at 450 °C, which is a high level for this temperature considering the maximum theoretical Li insertion capacity of anatase of 167 mAh/g (see Supporting Information Figure S6).[35] Furthermore, the material shows good cycling stability, which is comparable to other recently reported nanostructured titania systems (see Supporting Information Figure S7).[36,37]

In addition to the high capacitance, the nanocrystalline and mesoporous nature of the films also leads to a significant increase in the insertion/extraction rate of Li ions (Figure 7, and Supporting Information Figure S8). During a charging time of only 150 s, the microwave treated samples reach over 80% of their maximum insertion capacity, whereas reference films assembled from 20 nm anatase particles take approximately 10 times longer to reach that level. Similar accelerated kinetics were also described for films assembled from crystalline anatase nanoparticles[36,38] and were attributed to a significant contribution of pseudocapacitive processes in the total electrochemical Li insertion due to the large surface area of the nanoparticles. The small crystal size comparable to a maximum penetration depth for Li ions, the good connectivity of the crystals providing a continuous pathway for the ion/electron diffusion in the titania scaffold, and the excellent accessibility of the pore system for the Li ions in the electrolyte also contribute to the fast insertion kinetics of the prepared films.[38] The high insertion capacity and fast insertion kinetics in combination with a fast and facile preparation procedure make the described mesoporous films promising electrode materials for thin layer Li ion batteries and supercapacitors.

Conclusion

Nonaqueous sol−gel procedures using benzyl alcohol have been successfully employed for the preparation of crystalline metal oxide nanoparticles. However, for titania nanoparticles obtained with this method the dispersibility in organic solvents is limited and very small particle sizes are not accessible. Here we show that the combination of the new reaction medium *tert*-butanol and microwave irradiation using very short reaction times provides an effective synthesis protocol for the preparation of stable, soluble, and ultrasmall anatase nanoparticles. Additionally, due to the low boiling point of *tert*-butanol and the high solubility of Pluronic templates in this solvent, it was possible to develop a direct coating technique for the preparation of mesoporous films from nanocrystalline particles, omitting the time-consuming steps of centrifugation and redispersion of nanoparticles in a different solvent. The use of these ultrasmall and highly soluble particles allowed the production of mesoporous layers from nanoparticulate precursors using commercial Pluronic templates in an efficient one-pot procedure, and the films exhibit uniform mesoporous networks with a very high surface area. The films from microwave-treated titanium dioxide precursors can be converted, contrary to untreated *tert*-butanol sol−gel derived films, into anatase upon calcination at 450 °C due to a seeding effect of the previously formed crystalline nanoparticles. Finally, electrochemical lithium insertion in these films shows the advantages of the microwave treatment regarding the retention of mesoporosity and crystallinity, leading to high insertion capacities and remarkably fast charging rates. The efficient preparation of the ultrasmall nanoparticles and their applicability in the direct preparation of mesoporous titanium dioxide make this *tert*-butanol system an attractive alternative to other nonaqueous sol−gel strategies.

Experimental Section

Titanium dioxide nanoparticles were synthesized using a nonaqueous sol−gel route in *tert*-butyl alcohol under microwave irradiation. All chemicals were purchased from Sigma-Aldrich and used as received. *tert*-Butyl alcohol was dried over a 4 Å molecular sieve at 28 °C and filtered prior to use.

For all syntheses, titanium tetrachloride (1.5 mL, 13.7 mmol) was dissolved in toluene (10 mL) and added to *tert*-butyl alcohol (30 mL, 320 mmol) under continuous stirring. This solution was directly used as a metal oxide precursor for the sample tBuOH-SG. For the sample T60, this solution was kept at 60 °C for 24 h.

(35) Fattakhova-Rohlfing, D.; Wark, M.; Brezesinski, T.; Smarsly, B. M.; Rathouský, J. *Adv. Funct. Mater.* **2007**, *17*, 123–132.
(36) Brezesinski, T.; Wang, J.; Polleux, J.; Dunn, B.; Tolbert, S. H. *J. Am. Chem. Soc.* **2009**, *131*, 1802–1809.
(37) Ren, Y.; Hardwick, L. J.; Bruce, P. G. *Angew. Chem., Int. Ed.* **2010**, *49*, 2570.
(38) Wang, J.; Polleux, J.; Lim, J.; Dunn, B. *J. Phys. Chem. C* **2007**, *111*, 14925–14931.

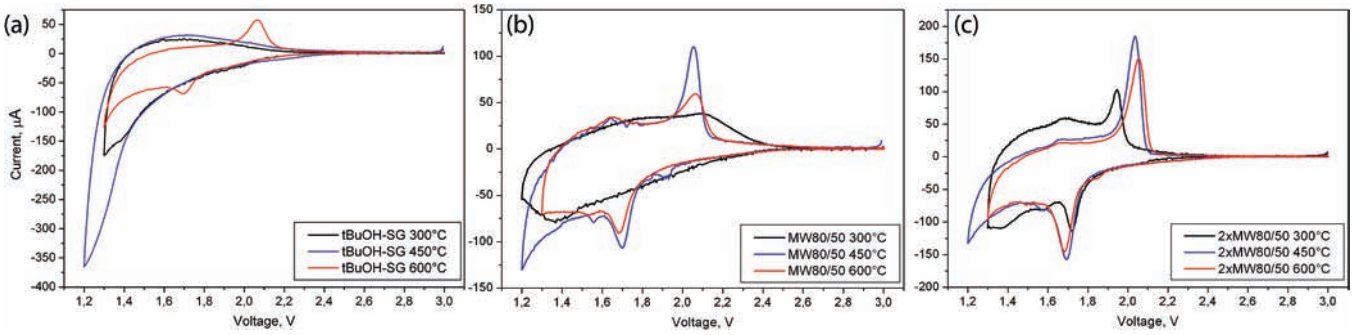

Figure 6. Cyclic voltammograms (scan rate 0.5 mV/s) from Li insertion of the mesoporous TiO_2 films after calcination at different temperatures: tBuOH-SG (a), MW80/50 (b), and 2xMW80/50 (c). Black: 300 °C; blue: 450 °C; red: 600 °C.

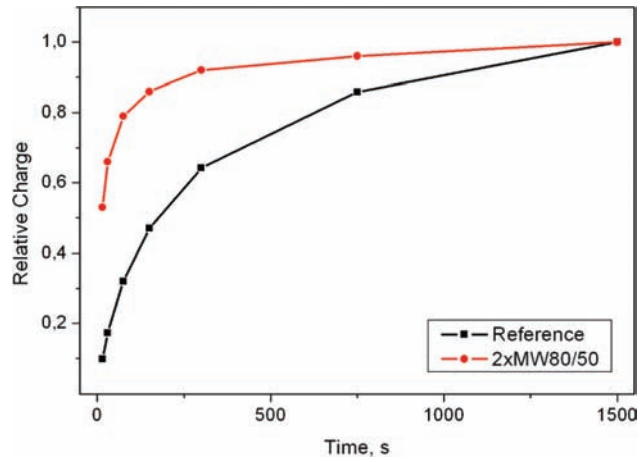

Figure 7. Comparison of charging rates for reaching maximum Li insertion into TiO_2 films assembled from different titania precursors. The relative charge was calculated as the ratio of measured charge over the maximum charge at the lowest scan rate. Black: Standard reference film made from 20 nm anatase particles, red: 2xMW80/50.

Microwave heating was performed in microwave autoclaves with an initial heating power of 1200 W (Synthos 3000, Anton Paar). MW50 was heated to 50 °C within 1 min and kept at this temperature for 1 h. MW80/50 was heated to 80 °C within 1 min and then kept at 50 °C for 20 min resulting in a slightly yellow, transparent solution of nanoparticles.

To obtain the fully crystalline nanoparticles, this heating procedure had to be repeated one more time after a cooling period to room temperature (2xMW80/50). The solution was then colorless, and titanium dioxide could be flocculated by the addition of *n*-heptane (*n*-heptane:*tert*-butanol/toluene 1:1 volume ratio) and separated by centrifugation at 50 000 rcf for 15 min. The content of TiO_2 of the resulting solid was determined to be 73 wt % by thermogravimetric analysis (Netzsch STA 440 C TG/DSC).

One-pot coating solutions were made by mixing the reaction mixtures with Pluronic P123 (1.4 g, 0.24 mmol) after microwave heating. Coatings with the nanocrystalline solid as a TiO_2 source were made by dissolving the amount of 0.2 g of nanoparticles in ethanol (2 mL) and mixing this solution with Pluronic P123 (0.2 g, 0.04 mmol) in THF (2 mL). Films of mesoporous TiO_2 were prepared on glass, FTO, or silicon by spin-coating with 1000 rpm at 23 ± 2 °C and a relative humidity of 45 ± 10%.

Scanning electron microscopy (SEM) was performed on a JEOL JSM-6500F scanning electron microscope equipped with a field emission gun, at 4 kV. High Resolution Transmission Electron Microscopy (HRTEM) and Scanning Transmission Electron Microscopy in High Angle Annular Dark Field mode (STEM-HAADF) were performed using an FEI Titan 80-300 equipped with a field emission gun operated at 300 kV. The particulate samples were prepared by evaporating a drop of a diluted solution of particles with small amounts of Pluronic P123 in THF on a Plano holey carbon coated copper grid. HRTEM of films was carried out by scraping the thin-film samples off the substrate onto a holey carbon coated copper grid or by direct spin-coating of the dilute solution on a nonholey carbon coated copper grid.

The porosity of the films was determined by the analysis of adsorption isotherms of Kr at the boiling point of liquid nitrogen (approximately 77 K) using an ASAP 2010 apparatus (Micromeritics). Textural data were obtained by comparing the shape of the hysteresis loop and the limiting adsorption at saturation pressure of the krypton sorption isotherms with reference materials (anatase powders) characterized by nitrogen sorption. Comparison plots were constructed for each sample, and the differentiation of these plots provided the basis for the pore size distribution.

X-ray diffraction analysis was carried out in reflection mode using a Scintag XDS 2000 (Scintag Inc.) and a Bruker D8 Discover with Ni-filtered Cu Kα radiation and a position-sensitive detector (Vantec). The thermal development of the XRD diffraction patterns was monitored by either ex situ heating or in in situ measurements using a DHS-1100 heating chamber with a graphite dome (Anton Parr).

Dynamic light scattering (DLS) was performed using a Malvern Zetasizer-Nano equipped with a 4 mW He−Ne laser (633 nm) and an avalanche photodiode detector. The scattering data were weighted based on particle number. Prior to DLS measurements, the viscosity of the solvent mixture was measured using a Bohlin rotational rheometer (Malvern).

For lithium insertion, the mesoporous films were coated on conductive ITO glass and subjected to cyclic voltammetry using a Parstat 2273 potentiostat (Princeton Applied Research). The measurements were performed in a 1 M solution of $LiN(SO_2CF_3)_2$ in a 1:1 w/w mixture of ethylenecarbonate and 1,2-dimethoxyethane. The solution preparation and cell assembly were carried out in an Ar-filled glovebox with a water and oxygen content of less than 20 ppm. The electrolyte solution was dried over a 4 Å molecular sieve. Li wire was used as both the auxiliary and the reference electrode. The working electrode was masked with a silicone resin to precisely define the exposed surface area. Electrochemical measurements were taken in a potential range from 3.0 to 1.3 V vs. Li. The scan rate in cyclic voltammetry measurements were varied from 0.5 to 100 mV s^{-1}. The weight of the titania layers was calculated using the thickness of the films and their density, which can be obtained by multiplying the density of anatase (3.9 g/cm^3) with the porosity determined by Kr sorption experiments. The accuracy of this method was confirmed by weighing 10 films of the same samples on larger substrates with similar film thicknesses. The reference sample for Li insertion was made as described elsewhere.[39] In brief, anatase nanoparticles of 20 nm size were synthesized hydrothermally and were mixed with cellulose binders. Porous films on FTO substrates were obtained using the doctor blade technique (Zehntner ZAA2300) and calcination at 450 °C for 30 min (1 °C/min ramp).

(39) Ito, S.; Murakami, T. N.; Comte, P.; Liska, P.; Grätzel, C.; Nazeeruddin, M. K.; Grätzel, M. *Thin Solid Films* **2008**, *516*, 4613–4619.

Acknowledgment. This work was supported by the Nanosystems Initiative Munich (NIM), by LMUexcellent funded by the DFG in Germany, and by the Elite Network of Bavaria (International Doctorate Program NanoBioTechnology). J.R. and V.K. are grateful to the Grant Agency of the Czech Republic (Grant No. 104/08/0435-1). The authors thank Benjamin Mandlmeier, Dr. Steffen Schmidt, and Dr. Markus Döblinger for SEM and TEM measurements.

Supporting Information Available: Characterization of nanoparticles and mesoporous films (TGA, SEM, SAXS, WAXS, Kr sorption, lithium insertion). This material is available free of charge via the Internet at http://pubs.acs.org.

JA101810E